High thermal stability of carbon-coated $L1_0$-FePt nanoparticles prepared by salt-matrix annealing

Chuan-Bing Rong,[1,a)] Narayan Poudyal,[1] Girija S. Chaubey,[1] Vikas Nandwana,[1] Yuzi Liu,[1] Y. Q. Wu,[2] M. J. Kramer,[2] M. E. Kozlov,[3] R. H. Baughman,[3] and J. Ping Liu[1,b)]
[1] *Department of Physics, University of Texas at Arlington, Arlington, Texas 76019, USA*
[2] *Ames Laboratory and Department of Materials Science and Engineering, Iowa State University, Ames, Iowa 50011, USA*
[3] *NanoTech Institute, University of Texas at Dallas, Richardson, Texas 75083, USA*

(Presented on 6 November 2007; received 7 September 2007; accepted 23 October 2007; published online 8 February 2008)

Monodisperse $L1_0$-FePt nanoparticles with size ranging from 3 to 8 nm were prepared by the salt-matrix annealing method. It was observed that the annealed particles have high thermal stability—no sintering occurred even when the particles were heated at 1100 °C for an hour. This high thermal stability resulted from carbon coating of the particles during salt-matrix annealing as consequence of decomposition of surfactants.

© *2008 American Institute of Physics*. [DOI: 10.1063/1.2832506]

I. INTRODUCTION

FePt nanoparticles are of great interest for the potential applications in ultrahigh density magnetic recording media and nanocomposite permanent magnets.[1,2] Due to the high magnetocrystalline anisotropy (7×10^6 J/m^3), $L1_0$-FePt particles are ferromagnetic even when as small as a few nanometers.[3–5] However, the as-synthesized FePt nanoparticles have a disordered $A1$ structure and are therefore superparamgnetic at room temperature. High temperature annealing is necessary to realize phase transformation from $A1$ to $L1_0$ structure. The annealing, however, always leads to serious particle agglomeration and sintering. Though dopants have been used to reduce the phase transition temperature, they also result in enhanced grain growth.[6–8] Direct chemical synthesis of $L1_0$-FePt nanoparticles has also been explored but only limited magnetic hardening was acheived.[9,10] Alternatively, SiO$_2$ coating of FePt particles has been used to prevent particle sintering during the high-temperature magnetic hardening process.[11] Recently, our group developed a salt-matrix annealing method that produced monodisperse $L1_0$-FePt nanoparticles having coercivity above 3 T.[12,13] In this work, we report unexpectedly high thermal stability of the monodisperse $L1_0$-FePt nanoparticles prepared by the salt-matrix method, which is technologically important for many applications. Our study indicates that the high temperature stability originates from the formation of a carbon shell due to the decomposition of surfactants during the salt-matrix annealing process.

II. EXPERIMENT

The face-centered-cubic (fcc) structure FePt nanoparticles with size ranging from 3 to 8 nm were synthesized by standard airless techniques with adjustable synthesis parameters.[13,14] 100 g salt powders (NaCl) were ball milled with 20 ml olyelamine for 24 h to reach a particle size smaller than 20 μm before they were mixed with the fcc FePt nanoparticles. The large weight ratio (400:1) of the salts to the fcc nanoparticles was chosen to separate the particles. The mixtures were then annealed at 700 °C for 4 h under forming gas with 93% Ar+7% H$_2$. After annealing, the salts were removed from the samples by washing the mixtures in de-ionized water and the solid residue was extracted by centrifugation. The dry nanoparticles without salt were then annealed at high temperatures ranging from 700 to 1100 °C to test their thermal stability. The structures were determined by transmission electron microscopy (TEM) and powder x-ray diffraction (XRD) with Cu $K\alpha$ radiation. The composition was checked by inductively coupled plasma–optical emission spectroscopy and energy dispersive spectroscopy (EDS). Magnetic properties were characterized using a superconducting quantum interference device magnetometer with field strength up to 7 T before and after the thermal stability measurements for the FePt nanoparticles.

III. RESULTS AND DISCUSSIONS

Structural characterizations of the salt-matrix annealed $L1_0$ nanoparticles have been reported in our previous work.[12–14] Figures 1(a) and 1(b) show the morphology of the

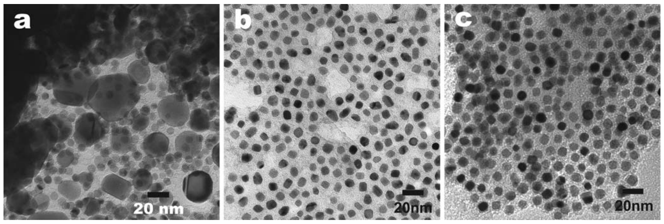

FIG. 1. TEM images of the 8 nm nanoparticles annealed in salt matrix at 700 °C for 4 h with a salt-to-particle ratio of (a) 20:1 and (b) 400:1. (c) The $L1_0$-FePt nanoparticles after washing out the salt and annealing at 1100 °C for 1 h.

[a)] Electronic mail: crong@uta.edu.
[b)] Electronic mail: pliu@uta.edu.

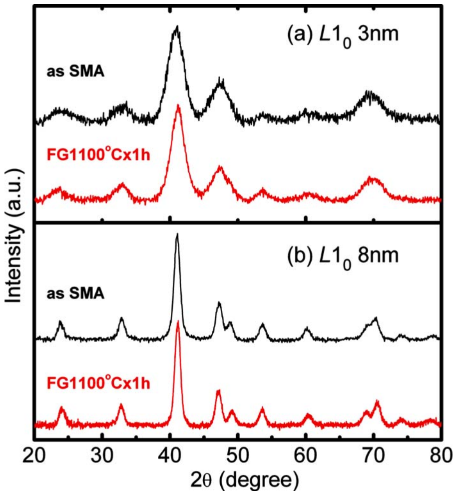

FIG. 2. (Color online) XRD patterns the $L1_0$ nanoparticles prepared by salt-matrix annealing method before and after annealing at 1100 °C for 1 h for (a) 3 nm and (b) 8 nm.

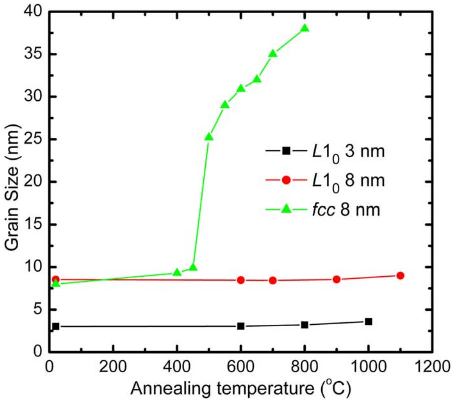

FIG. 3. (Color online) Dependence of grain (particle) size of the salt-matrix annealed $L1_0$ particles and fcc nanoparticles on the annealing temperature.

8 nm FePt particles after annealing at 700 °C for 4 h with salt-to-FePt mass ratio of 20:1 and 400:1, respectively. It was found that the latter conditions resulted in formation of nearly monodisperse $L1_0$-FePt nanoparticles. Large particles of about 50 nm in diameter and over were often observed in compositions with 20:1 salt-to-FePt ratio probably because of particle sintering. This indicates the importance of the particle separation media. Moreover, a continuous polycrystalline structure forms if there is no salt acting as the particle separator. Surprisingly, also the monodisperse $\mathrm{L1_0}$-FePt nanoparticles are stable even after annealing at 1100 °C for 1 h. As shown in Fig. 1(c), there is no particle sintering and grain growth but the formation of more regular shape after the high temperature annealing.

Figure 2 shows the XRD patterns of the 3 and 8 nm salt-matrix annealed nanoparticles before and after annealing under forming gas at different temperatures. The grain size (determined using Scherrer formula) of the salt-matrix annealed particles is around 3.0 ± 0.1 and 8.4 ± 0.2 nm, respectively. The equal grain size and particle size could be an evidence of the single crystalline nature of both 3 and 8 nm FePt particles after salt-matrix annealing. The $L1_0$ nanoparticles are very stable at temperature up to 1100 °C even after removing the salt matrix. The grain (or particle) size only increases to 3.4 ± 0.1 and 8.9 ± 0.2 nm for the 3 and 8 nm nanoparticles after heated at 1100 °C for 1 h, respectively. Figure 3 summarizes the dependence of grain size (or particle size) on the annealing temperature. The XRD analysis agrees with the TEM results that exhibit high temperature stability of the salt-matrix annealed $L1_0$-FePt particles, while the sintering of fcc nanoparticles are serious.

It has been reported that the oleylamine surfactant mostly decomposes at about 400 °C.[15–17] Therefore, we hypothesized that carbon shells form around the FePt particles as a result of this pyrolysis of the surfactant during salt-matrix annealing at 700 °C, especially since a large amount of oleylamine was used in this work to separate the salt and nanoparticles. Figure 4 shows a high-resolution TEM image of the salt-matrix annealed 8 nm particles. A lattice-fringe distance of about 0.22 nm observed in the FePt particles is typical for interplanar distance of (111) in $L1_0$-FePt phase. Around the surface of the particles, a lattice fringe distance of 0.35 nm is observed due to a light element coating, which appears due to graphitic carbon. This carbon shell can act as the diffusion barrier layer during the annealing, thereby impeding sintering of the FePt nanoparticles. The structural lattice parameters of the $L1_0$-FePt nanoparticles are about the same ($a = 0.3855$ nm and $c = 0.3757$ nm) before and after annealing at 1100 °C for 1 h, which confirms that no carbon diffusion from the shell to the FePt particles during the high-temperature annealing.

To further prove the carbon layer is on the surface of the particles, Raman spectra were collected. Figure 5 shows the Raman spectra of the salt-matrix annealed 4 and 8 nm FePt nanoparticles. It was found that both samples have similar patterns. There are two major peaks around 1320 and 1580 $\mathrm{cm^{-1}}$ which are attributed to the amorphous carbon and graphite, respectively.[18] EDS then gave a rough determination the carbon content in the salt-matrix annealed particles with different sizes. It confirms the existence of 15–25 wt % carbon in the salt-matrix annealed samples. It should be noted that the carbon content can be controlled by the amount of the added surfactants in the salt matrix.

The morphology change of salt-matrix annealed $L1_0$ particles can be checked indirectly by evaluating exchange coupling interaction, such as remanence enhancement and Henkel plot. The Henkel plot was measured as $\delta m(H) = m_d(H) - [1 - 2m_r(H)]$, where m_d and m_r are the normalized dc de-

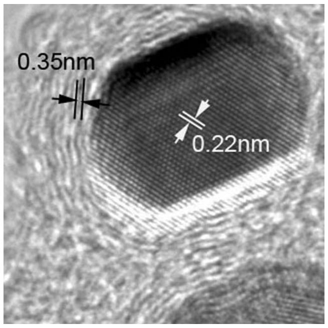

FIG. 4. High-resolution TEM image of the 8 nm salt-matrix annealed $L1_0$ particles.

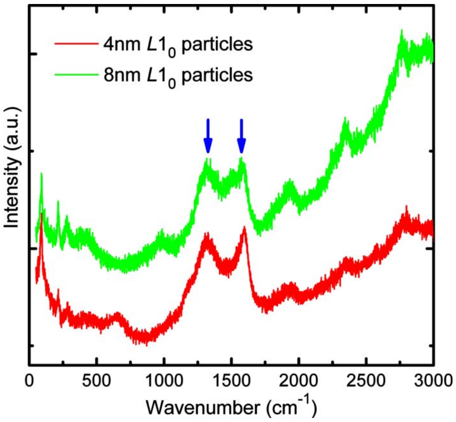

FIG. 5. (Color online) Raman spectra of the salt-matrix annealed 4 and 8 nm FePt nanoparticles.

magnetization remanence and isothermal magnetization remanence.[19–22] Positive and negative δm values are assumed to be attributed to magnetic exchange coupling and magnetic dipolar interaction, respectively. Figure 6 shows the $\delta m(H)$ plots of 8 nm salt-matrix annealed particles before and after annealing at 1000 °C for an hour. It was found that all δm values are negative and the $\delta m(H)$ curves are similar for the particles before and after high-temperature annealing. This means the magnetic dipolar interactions dominate the demagnetization process for the particles even after the high-temperature annealing. In other words, there is no sintering in the $L1_0$ particles otherwise, the δm values should have increased and become positive due to the interparticle (or intergrain) exchange coupling.

It was noted that the demagnetization loops of the $L1_0$ nanoparticles are smoother after annealing at 1100 °C for an hour but the improvement is not significant. This is most likely due to an increase in the phase transition for partially ordered nanoparticles after the salt-matrix annealing. For example, the chemical ordering parameters can be calculated by the equation $S \cong 0.85(I_{001}/I_{002})^{1/2}$, where I_{hkl} is the integrated intensity of (hkl) XRD peak of $L1_0$-FePt nanoparticles.[11,23,24] For 8 nm $L1_0$ particles, S was found to increase from 0.88 to 0.92 as a result of the high-temperature annealing.

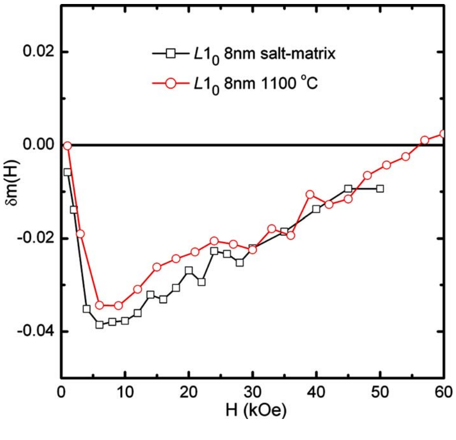

FIG. 6. (Color online) Henkel plot of the 8 nm nanoparticles before and after annealing at 1000 °C for 1 h.

IV. CONCLUSIONS

The monodisperse $L1_0$-FePt nanoparticles with 3–8 nm particle size prepared by the salt-matrix method are highly thermally stable even at 1100 °C. High-resolution transmission electron microscopy, Raman spectra, energy dispersive spectra, and magnetic measurement suggest that the $L1_0$-FePt nanoparticles were coated by carbon shell after salt-matrix annealing.

ACKNOWLEDGMENTS

This work was supported by U.S. DoD/MURI under Grant No. N00014-05-1-0497 and DARPA through ARO under Grant No. DAAD 19-03-1-0038. Work at the Ames Laboratory was supported by the Department of Energy, Basic Energy Sciences under Contract No. DE-AC02-07CH11358.

[1] S. Sun, C. B. Murray, D. Weller, L. Folks, and A. Moser, Science **287**, 1989 (2000).
[2] C. B. Rong, H. W. Zhang, X. B. Du, J. Zhang, S. Y. Zhang, and B. G. Shen, J. Appl. Phys. **96**, 3921 (2004).
[3] Q. A. Ivanov, L. V. Solina, V. A. Demshima, and L. M. Maget, Phys. Met. Metallogr. **35**, 81 (1973).
[4] D. Weller, A. Moser, L. Folks, M. E. Bet, W. Lee, M. Toney, M. Schwieckert, J.-U. Thiele, and M. F. Doerner, IEEE Trans. Magn. **36**, 10 (2000).
[5] C. B. Rong, V. Nandwana, N. Poudyal, J. P. Liu, M. E. Kozlov, and R. H. Baughman, Y. Ding, and Z. L. Wang, J. Appl. Phys. **102**, 023908 (2007).
[6] S. S. Kang, J. W. Harrell, and D. E. Nikles, Nano Lett. **2**, 1033 (2002).
[7] Q. Y. Yan, T. Kim, A. Purkayastha, P. G. Ganesan, M. Shima, and G. Ramanath, Adv. Mater. (Weinheim, Ger.) **17**, 2233 (2005).
[8] J. W. Harrell, D. E. Nikles, S. S. Kang, X. C. Sun, Z. Jia, S. Shi, J. Lawson, G. B. Thompson, C. Srivastava, and N. V. Seetala., Scr. Mater. **53**, 411 (2005).
[9] S. S. Kang, Z. Y. Jia, S. F. Shi, D. E. Nikles, and J. W. Harrell, J. Appl. Phys. **97**, 10J318 (2005).
[10] B. Jeyadevan, A. Hobo, K. Urakawa, C. N. Chinnasamy, K. Shinoda, and K. Tohji, J. Appl. Phys. **93**, 7574 (2003).
[11] S. Yamamoto, Y. Morimoto, T. Ono, and M. Takano, Appl. Phys. Lett. **87**, 032503 (2005).
[12] K. Elkins, D. Li, N. Poudyal, V. Nandwana, Z. Jin, K. Chen, and J. P. Liu, J. Phys. D **38**, 2306 (2005).
[13] C. B. Rong, D. R. Li, V. Nandwana, N. Poudyal, Y. Ding, Z. L. Wang, H. Zeng, and J. P. Liu, Adv. Mater. (Weinheim, Ger.) **18**, 2984 (2006).
[14] C. B. Rong, N. Poudyal, G. S. Chaubey, V. Nandwana, R. Skomski, Y. Q. Wu, M. J. Kramer, and J. P. Liu, J. Appl. Phys. **102**, 043913 (2007).
[15] Y. Sahoo, H. Pizem, T. Fried, D. Golodnitsky, L. Burstein, C. N. Sukenik, and G. Markovich, Langmuir **17**, 7907 (2001).
[16] Y. Ding, S. Yamamuro, D. Farrell, and S. A. Majetich, J. Appl. Phys. **93**, 7411 (2003).
[17] X. W. Wu, C. Liu, L. Li, P. Jones, R. W. Chantrell, and D. Weller, J. Appl. Phys. **95**, 6810 (2004).
[18] C. Kufazvinei, R. W. Leahy, S. M. Lipson, W. J. Blau, F. C. Dillon, T. R. Spalding, M. A. Morris, J. D. Holmes, G. Allan, and J. Patterson, Proc. SPIE **5824**, 149 (2005).
[19] K. O'Grady, M. El-Hilo, and R. W. Chantrell, IEEE Trans. Magn. **29**, 2608 (1993).
[20] A. Bollero, O. Gutfleisch, K.-H. Muller, L. Schultz, and G. Drazic, J. Appl. Phys. **91**, 8159 (2002).
[21] C. B. Rong, H. W. Zhang, B. G. Shen, and J. P. Liu, Appl. Phys. Lett. **88**, 042504 (2006).
[22] C. B. Rong, V. Nandwana, N. Poudyal, Y. Li, J. P. Liu, Y. Ding, and Z. L. Wang, J. Phys. D **40**, 712 (2007).
[23] B. E. Warren, *X-Ray Diffraction* (Dover, New York, 1990), Ch. 12.
[24] J. A. Christodoulides, P. Farber, M. Daniil, H. Okumura, G. C. Hadjipanayis, V. Skumryev, A. Simopoulos, and D. Weller, IEEE Trans. Magn. **37**, 1292 (2001).